

Uncertainty and Sensitivity Analysis of the Effective Reproduction Number for a Deterministic Mathematical Model for Tuberculosis-Schistosomiasis Co-infection Dynamics.

I. I. Ako

Department of Mathematics, University of Benin, Benin City, Nigeria

ARTICLE INFO

Article history:

Received xxxxx
 Revised xxxxx
 Accepted xxxxx
 Available online xxxxx

Keywords:

Tuberculosis,
 Schistosomiasis,
 Co-infection,
 Uncertainty
 Sensitivity.

ABSTRACT

We present the uncertainty and sensitivity analysis of the effective reproduction number for the deterministic mathematical model for tuberculosis-schistosomiasis co-infection dynamics as presented by Ako and Olowu [1]. The results from these contour plots suggest that the effect of the cercarial production, cercarial penetration, the number of schistosome eggs secreted and the successful conversion of the eggs to miracidia, on the hardship of tuberculosis in a populace, is predominantly determined by the medical care levels for individuals with active schistosomiasis. Hence, public health policy should take into account the level of medical care facilities available. With increasing (and sustained) treatment rates for schistosomiasis infections, having a large proportion of active schistosomiasis patients expeditiously receiving medical care will result in a reduction in the disease hardship in the populace.

1. Introduction

Tuberculosis, also known as known as TB, generated by the pathogen *Mycobacterium tuberculosis*, is a contagious malady whose propagation is airborne. TB was the leading contagious disease killer globally second only to COVID-19 in 2022 [43]. It ranked also as the number killer of people with HIV cum a major cause of mortality associated with antimicrobial resistance [43]. About 10.6 million persons took ill with the disease globally in 2022 where individuals living with HIV contributed 6.3% to the total number. TB was responsible for about 130 million deaths in 2022 which was inclusive of 167,000 HIV-infected persons. Eight nations contributed to more than two-third of the worldwide total [43]. Schistosomiasis, both an acute cum parasitic infection generated by trematode worms of the genus *Schistosoma* [44].

*Corresponding author: I. I. Ako

E-mail address: ignatius.ako@uniben.edu,

<https://doi.org/10.60787/tnamp.v20.378>

1115-1307 © 2024 TNAMP. All rights reserved

Human infection is possible via regular stay-at-home, agrarian, recreational and vocational activities which brings them in contact with water that is infested [44]. In 2021, 251.4 million persons were preventive medical intervention ([44]), of the which 75.3 million individuals reportedly received medical intervention with praziquantel, with 90% of them domiciled in Africa [44]. 78 nations of the world reported schistosomiasis infection transmission [44]. TB and schistosomiasis are co-endemic and co-infectious from global reports where the presence of schistosomiasis has the ability to regulate infection with TB (see [1] and the references therein). Several authors have rigorously investigated, through mathematical modelling, the disease dynamics of schistosomiasis and its co-infection with other diseases other than TB [3, 8, 10, 11, 14, 13, 16, 17, 18, 20, 21, 22, 23, 24, 32, 33, 34, 36, 37, 45, 46, 47] while several treatises on the mathematical investigation for the infection dynamics of TB other diseases other than schistosomiasis [2, 7, 25, 26, 30, 27, 28, 31, 29, ?, 41]. Only Ako and Olowu [1] had developed a deterministic mathematical model to analyze the co-infection dynamics of TB and schistosomiasis [1].

The purpose of this current study is to mathematically and numerically carryout uncertainty and sensitivity analysis of the effective reproduction number for the mathematical model of Ako and Olowu [1] with respect to certain parameters of interest.

The paper is organized as follows: Section 2 contains a review of the model formulation in [1]. The mathematical analysis of the effective reproduction number (both qualitative and quantitative) is done in Section 3. Section 4 contains the uncertainty and sensitivity analysis of certain key parameters to the effective reproduction number while Section 5 gives the conclusion.

2 Model Formulation

The TB-schistosomiasis co-infection transmission model under consideration was developed by [1] with all the assumptions, definitions and basic properties therein.

The model demarcates the entire human populace at time t , represented by $N_H(t)$, into fourteen mutually exclusive classes of susceptible to infections ($S_H(t)$), latent with TB but not infectious ($E_{HT}(t)$), active TB ($I_{HT}(t)$), exogenously re-infected with TB ($I_{RT}(t)$), treated for TB ($T_{HT}(t)$), exposed to schistosomiasis ($E_{HS}(t)$), infected with schistosomiasis ($I_{HS}(t)$), treated for schistosomiasis ($T_{HS}(t)$), exposed to TB, exposed to schistosomiasis ($E_{TS}(t)$), with active TB, exposed to schistosomiasis ($I_{ST}(t)$), exogenously re-infected with TB, exposed to schistosomiasis ($I_{RS1}(t)$), exposed to TB, with active schistosomiasis ($E_{ST}(t)$), exogenously re-infected with TB and active schistosomiasis ($I_{RS2}(t)$), and with active TB, active schistosomiasis ($I_{TS}(t)$). Where

$$\begin{aligned} N_H(t) = & S_H(t) + E_{HT}(t) + I_{HT}(t) + I_{RT}(t) + T_{HT}(t) + E_{HS}(t) \\ & + I_{HS}(t) + T_{HS}(t) + E_{TS}(t) + I_{ST}(t) + I_{RS1}(t) + E_{ST}(t) \\ & + I_{RS2}(t) + I_{TS}(t). \end{aligned} \quad (2.1)$$

Incorporating the pathogen responsible for schistosomiasis into the co-infection dynamics, we assume that the miracidia and cercariae population at the different stages in the life-cycle of the *Schistosoma spp* are depicted by $L(t)$ and $J(t)$ compartments respectively. Next, we incorporate the intermediary hosts, freshwater snails, for the pathogen responsible for schistosomiasis in the model construction. We presume that the entire snail populace in the freshwater environment at time t , given by $N_S(t)$, is broken down into the jointly exclusive classes of susceptible snails ($S_S(t)$) alongside snails penetrated with miracidia ($I_S(t)$), where

$$N_S(t) = S_S(t) + I_S(t). \quad (2.2)$$

I.I. Ako - Transactions of NAMP 20, (2024) 45-60

The model's associated parameters are tabulated in Table 1, while the values and ranges of the parameters used for numerical simulation on the model (2.3) are listed in Tables 3 and 4, respectively.

$$\begin{aligned}
S'_H &= \Lambda_H - \lambda_T S_H - \lambda_J S_H - \mu_H S_H, \\
E'_{HT} &= (1-p)\lambda_T(S_H + \xi T_{HT} + T_{HS}) + \zeta_{S1} E_{ST} - (1-\pi_1)\lambda_T E_{HT} \\
&\quad - \lambda_J E_{HT} - (\kappa_1 + \mu_H) E_{HT}, \\
I'_{HT} &= p\lambda_T(S_H + \xi T_{HT} + T_{HS}) + \kappa_1 E_{HT} + \zeta_{S3} I_{TS} - \lambda_J I_{HT} \\
&\quad - (\zeta_T + \delta_T + \mu_H) I_{HT}, \\
I'_{RT} &= (1-\pi_1)\lambda_T E_{HT} + \zeta_{S2} I_{RS2} - \lambda_J I_{RT} - (\zeta_R + \delta_R + \mu_H) I_{RT}, \\
T'_{HT} &= \zeta_T I_{HT} + \zeta_R I_{RT} - \xi \lambda_T T_{HT} - \lambda_J T_{HT} - \mu_H T_{HT}, \\
E'_{HS} &= \lambda_J(S_H + T_{HT} + \psi T_{HS}) + \zeta_{T1} I_{ST} + \zeta_{R1} I_{RS1} - \eta_1 \lambda_T E_{HS} \\
&\quad - (\alpha_1 + \mu_H) E_{HS}, \\
I'_{HS} &= \alpha_1 E_{HS} + \zeta_{T2} I_{RS2} + \zeta_{T3} I_{TS} - \eta_2 \lambda_T I_{HS} - (\zeta_S + \delta_S + \mu_H) I_{HS}, \\
T'_{HS} &= \zeta_S I_{HS} - \lambda_T T_{HS} - \psi \lambda_J T_{HS} - \mu_H T_{HS}, \\
E'_{TS} &= (1-m)\eta_1 \lambda_T E_{HS} + \lambda_J E_{HT} - (1-\pi_2)\lambda_T E_{TS} - (\alpha_2 + \kappa_2 + \mu_H) E_{TS}, \\
I'_{ST} &= m\eta_1 \lambda_T E_{HS} + \lambda_J I_{HT} + \lambda_J I_{RT} + \kappa_2 E_{TS} - (\zeta_{T1} + \sigma + \chi_1 \delta_T + \mu_H) I_{ST}, \\
I'_{RS1} &= (1-\pi_2)\lambda_T E_{TS} - (\alpha_3 + \zeta_{R1} + \tau_1 \delta_R + \mu_H) I_{RS1}, \\
E'_{ST} &= (1-f)\eta_2 \lambda_T E_{TS} + \alpha_2 E_{TS} - (1-\pi_3)\lambda_T E_{ST} - (\zeta_{T1} + \kappa_3 + \nu_1 \delta_S + \mu_H) E_{ST}, \\
I'_{RS2} &= (1-\pi_3)\lambda_T E_{ST} + \alpha_3 I_{RS1} - (\zeta_{T2} + \zeta_{S2} + \tau_2 \delta_R + \nu_2 \delta_S + \mu_H) I_{RS2}, \\
I'_{TS} &= f\eta_2 \lambda_T E_{TS} + \kappa_3 E_{ST} + \sigma I_{ST} - (\zeta_{T3} + \zeta_{S3} + \chi_2 \delta_T + \nu_3 \delta_S + \mu_H) I_{TS}, \\
L' &= N_e \gamma (I_{HS} + E_{ST} + I_{RS2} + I_{TS}) - \mu_L L, \\
S'_S &= \Lambda_S - \lambda_L S_S - \mu_S S_S, \\
I'_S &= \lambda_L S_S - \mu_S I_S, \\
J' &= \phi I_S - \mu_J J.
\end{aligned} \tag{2.3}$$

Table 1: Description of parameters of model (2.3) [1]

Parameter	Description
Λ_H	Human recruitment rate
μ_H	Natural death rate of humans
β_T	Tuberculosis transmission rate
ξ	Reduced rate of re-infection with TB after recovery from a previous infection
f, m, p	Fraction of fast progressors to TB
π_1, π_2, π_3	Exogenous re-infection rates
$\kappa_1, \kappa_2, \kappa_3$	Endogenous reactivation rates
$\zeta_T, \zeta_{T1}, \zeta_{T2}, \zeta_{T3}, \zeta_R, \zeta_{R1}$	Treatment rates for TB
δ_T, δ_R	TB-induced human death rates
ψ	Reduced rate of infection with schistosomiasis after recovery from a previous infection
α_1	Rate of progression from latently to actively infected with schistosomiasis
α_2	Rate of progression from exposed to both TB/schistosomiasis to exposed to TB/active schistosomiasis
α_3	Rate of progression from exogenously re-infected with TB/exposed to

I.I. Ako - Transactions of NAMP 20, (2024) 45-60

$\zeta_{S_1}, \zeta_{S1}, \zeta_{S2}, \zeta_{S3}$	schistosomiasis to exogenously re-infected with TB/active schistosomiasis
δ_S	Treatment rates for schistosomiasis
σ	Schistosomiasis-induced human death rate
χ_1, χ_2	Rate of progression from active TB/exposed to schistosomiasis to active TB/active schistosomiasis
η_1, η_2	Adjustment parameters for increased TB mortality due to co-infection
Θ_{RT}	Adjustment parameters which account for the increased susceptibility to TB of humans with latent and active schistosomiasis
$\Theta_{RS1}, \Theta_{RS2}$	Adjustment parameters which account for the decreased probability of transmission of TB by humans exogenously re-infected with TB
Π_1, Π_2	Adjustment parameters which account for the increased probability of transmission of TB by humans exogenously re-infected with TB, and exposed to/active schistosomiasis, respectively
τ_1, τ_2	Adjustment parameters which account for the increased probability of infectiousness of humans with active TB and latent/active schistosomiasis respectively
v_1, v_2, v_3	Adjustment parameters for increased TB mortality as a result of exogenous re-infection due to co-infection
Λ_S	Adjustment parameters which account for schistosomiasis-induced deaths
μ_S	Recruitment rate for snail population
ε	Snail mortality rate
L_0	Limitation of the growth velocity
β_L	Saturation constant for the miracidia
N_e	Miracidial infection rate
γ	Number of eggs secreted by humans
μ_L	Rate at which eggs successfully become miracidia
ϕ	Miracidial death rate
J_0	Cercarial production rate
β_J	Saturation constant for the cercariae
μ_J	Cercarial infection rate
	Cercarial death rate

where the force of infection associated with TB, schistosomiasis (following penetration by cercariae) and snail penetration by miracidia respectively is given below:

$$\lambda_T = \frac{\beta_T (I_{HT} + \Theta_{RT} I_{RT} + \Theta_{RS1} I_{RS1} + \Theta_{RS2} I_{RS2} + \Pi_1 I_{ST} + \Pi_2 I_{TS})}{N_H}, \quad (2.4)$$

$$\lambda_J = \frac{\beta_J J}{J_0 + \varepsilon J}, \quad (2.5)$$

$$\lambda_L = \frac{\beta_L L}{L_0 + \varepsilon L}. \quad (2.6)$$

3 Analysis of the Effective Reproduction, \mathcal{R}_{TS} , obtained in [1]

The model system (2.3) in [1] possesses a DFE represented by

$$\begin{aligned} E_0 &= (S_H^*, E_{HT}^*, I_{HT}^*, I_{RT}^*, T_{HT}^*, E_{HS}^*, I_{HS}^*, T_{HS}^*, E_{TS}^*, I_{ST}^*, I_{RS1}^*, E_{ST}^*, I_{RS2}^*, I_{TS}^*, L^*, S_S^*, I_S^*, J^*) \\ &= \left(\frac{\Lambda_H}{\mu_H}, 0, 0, 0, 0, 0, 0, 0, 0, 0, 0, 0, 0, 0, 0, 0, \frac{\Lambda_S}{\mu_S}, 0, 0 \right) \end{aligned}$$

where the associated effective reproduction number of the model (2.3), R_{TS} , obtained via the next-generation operator method [40], is given by

$$\mathfrak{R}_{TS} = \max\{\mathfrak{R}_{HT}, \mathfrak{R}_{HS}\} \quad (3.1)$$

where

$$\mathfrak{R}_{HT} = \frac{\beta_T((1-p)\kappa_1 + p(\kappa_1 + \mu_H))}{(\kappa_1 + \mu_H)(\zeta_T + \delta_T + \mu_H)}, \quad \mathfrak{R}_{HS} = \sqrt{\frac{\alpha_1\beta_J\beta_L\Lambda_H\Lambda_S N_e\gamma\phi}{J_0 L_0 \mu_H \mu_J \mu_L \mu_s^2 (\alpha_1 + \mu_H)(\zeta_S + \delta_S + \mu_H)}}$$

3.1 Analysis of \mathfrak{R}_{TS}

Evaluation of the threshold quantity, \mathfrak{R}_{TS} , analogous to some key parameters ($\zeta_T, \zeta_S, N_e, \gamma, \phi, J_0$ and L_0) is investigated by considering the partial derivatives of \mathfrak{R}_{TS} corresponding to these parameters. We proceed to plot the contour plots of employing (3.1) using the parameter values in Tables 2 and 3.

3.1.1 Analysis of \mathfrak{R}_{HT}

Calculating the partial derivatives of \mathfrak{R}_{HT} relative to one of the parameters under scrutiny (ζ_T) exposes the consequence of this parameter on TB regulation in the populace. This implies that

$$\frac{\partial \mathfrak{R}_{HT}}{\partial \zeta_T} = -\frac{\mathfrak{R}_{HT}}{(\zeta_T + \delta_T + \mu_H)} < 0 \quad (3.2)$$

Apparently, it ensues from (3.2) that the partial derivative is negative, unconditionally. Thus, adequate medical care rate of TB at the phase of infection will exert a positive influence in decreasing the load of TB among the populace, regardless of the rates of the additional parameters in the expression on the right flank of (3.2).

We further investigate the sensitivity analysis of \mathfrak{R}_{HT} to treatment. Thus, we consider the limiting value of \mathfrak{R}_{HT} as this extremely large value is assigned to this particular parameter under investigation. If we consider the limiting value of \mathfrak{R}_{HT} as $\zeta_T \rightarrow \infty$, we obtain

$$\lim_{\zeta_T \rightarrow \infty} R_{HT} = 0 \quad (3.3)$$

The limiting value in (3.3) demonstrates the impact of a tuberculosis regulation policy or programme which concentrates on adequate and prompt treatment of humans with infectious TB among the populace provided that policy leads to a significant decline in the corresponding effective reproduction number, \mathfrak{R}_{HT} , to a value below one. From the analysis of R_{HT} as seen in (3.2) and (3.3), respectively, we obtain the following result:

Lemma 3.1. *Effective treatment rate (ζ_T) for the infectious phase of infection will have a positive impact in decreasing the tuberculosis load among the populace, regardless of the rates of the additional parameters in the effective reproduction number.*

Further analysis of the threshold quantity, \mathfrak{R}_{HT} , is carried out by investigating its sensitivity to certain key parameters, namely: the treatment rate (ζ_T), the transmission rate (β_T), endogenous reactivation rate (κ_1) as well as the fraction or proportion of fast progressors to TB (p). Hence, we examine the contour plots (Figures 1 - 2) of \mathfrak{R}_{HT} as functions of $\zeta_T, \beta_T, \kappa_1$ and p . The values of the parameters used for generating the contour plots are obtained from Tables 3 and 4.

The plot in Figure 1 indicates that effective treatment of about 80% of infectiously-infected humans (with a medical care rate of $\zeta_T = 0.75$ and a disease transmission rate $\beta_T = 1.2$) is needed in order to annihilate tuberculosis from the populace. Any regulatory policy dependent on the measures presented in Figure 1 will compel \mathfrak{R}_{HT} to acquire a value below unity.

Figure 2 implies that effective treatment of about 77% of actively-infected individuals via endogenous reactivation (with a treatment rate of $\zeta_T = 0.75$, endogenous reactivation rate of $\kappa_1 = 0.05$ and a disease transmission rate $\beta_T = 1.2$) is needed to annihilate tuberculosis from the populace. Any regulatory policy dependent on the measures presented in Figure 2 will compel \mathfrak{R}_{HT} to acquire a value below one.

The results from these contour plots suggest that the effect of the proportion of active TB infections and the fraction of infectious tuberculosis cases via endogenous reactivation, on the weight of tuberculosis in a populace, is predominantly determined by the medical care levels for humans with tuberculosis. Hence, public health policy should take into cognizance the level of medical care facilities for the management of infectious TB cases in the populace. With increasing (and sustained) medical care rates for TB infections, having a large proportion of infectious tuberculosis patients expeditiously receiving medical care will result in a decline in the disease hardship in the populace.

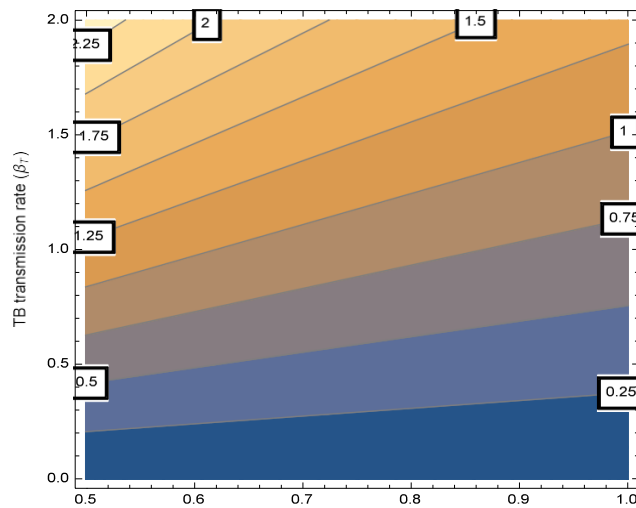


Figure 1: Contour plot consisting of \mathfrak{R}_{HT} dependent on ζ_T and β_T

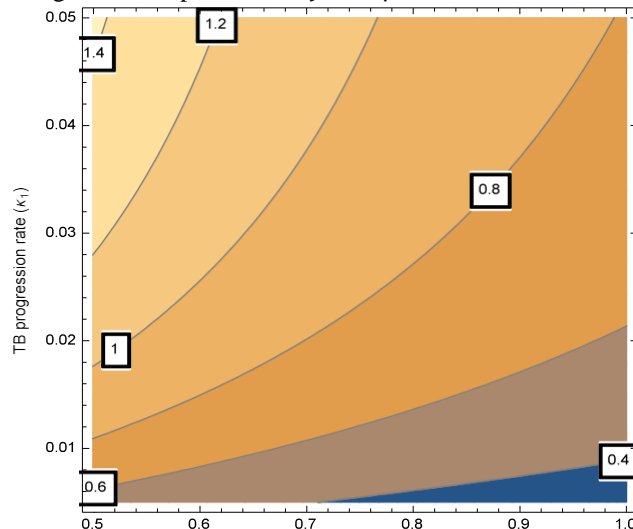


Figure 2: Contour plot consisting of R_{HT} dependent on ζ_T and κ

3.1.2 Analysis of \mathfrak{R}_{HS}

Calculating the partial derivatives of \mathfrak{R}_{HS} relative to the parameters under scrutiny (ζ_S , N_e , γ , ϕ , J_0 and L_0) further exposes the influence of these parameters on schistosomiasis control in the community. This gives

$$\frac{\partial \mathfrak{R}_{HS}^2}{\partial \zeta_S} = -\frac{\alpha_1 \beta_J \beta_L \Lambda_H \Lambda_S N_e \gamma \phi}{2J_0 L_0 \mu_H \mu_J \mu_L \mu_s^2 (\alpha_1 + \mu_H) (\zeta_S + \delta_S + \mu_H)^2 \mathfrak{R}_{HS}} < 0 \quad (3.4)$$

Apparently, it ensues from (3.4) that the partial derivative is negative, unconditionally. Thus, effective medical care rate of schistosomiasis at the phase of infection will exert a positive impact in decreasing the weight of schistosomiasis in the populace, regardless of the rates of the additional parameters in the expression on the right flank of (3.4).

$$\frac{\partial \mathfrak{R}_{HS}^2}{\partial N_e} = \frac{\alpha_1 \beta_J \beta_L \Lambda_H \Lambda_S \gamma \phi}{2J_0 L_0 \mu_J \mu_L \mu_s^2 (\alpha_1 + \mu_H) (\zeta_S + \delta_S + \mu_H)^2 \mathfrak{R}_{HS}} > 0 \quad (3.5)$$

However, we observe, from (3.5), that the number of schistosome eggs secreted by infectious human sub-population will exert a negative influence in decreasing the weight of schistosomiasis in the populace, regardless of the rates of the additional parameters in the expression on the right flank of (3.5).

$$\frac{\partial \mathfrak{R}_{HS}^2}{\partial \gamma} = \frac{\alpha_1 \beta_J \beta_L \Lambda_H \Lambda_S N_e \phi}{2J_0 L_0 \mu_J \mu_L \mu_s^2 (\alpha_1 + \mu_H) (\zeta_S + \delta_S + \mu_H)^2 \mathfrak{R}_{HS}} > 0 \quad (3.6)$$

We also observe, from (3.6), that the rate at which schistososome eggs (secreted by infectious human sub-population) successfully become miracidia will exert a negative influence in decreasing the weight of schistosomiasis in the community, regardless of the rates of the additional parameters in the expression on the right flank of (3.6).

$$\frac{\partial \mathfrak{R}_{HS}^2}{\partial \phi} = \frac{\alpha_1 \beta_J \beta_L \Lambda_H \Lambda_S N_e \gamma}{2J_0 L_0 \mu_J \mu_L \mu_s^2 (\alpha_1 + \mu_H) (\zeta_S + \delta_S + \mu_H) \mathfrak{R}_{HS}} > 0 \quad (3.7)$$

We further observe, from (3.7), that the cercarial production rate (by the infectious snail sub-population) will exert a negative influence in decreasing the weight of schistosomiasis in the populace, regardless of the rates of the additional parameters in the expression on the right flank of (3.7).

$$\frac{\partial \mathfrak{R}_{HS}^2}{\partial J_0} = -\frac{\alpha_1 \beta_J \beta_L \Lambda_H \Lambda_S N_e \phi}{2J_0 L_0 \mu_J \mu_L \mu_s^2 (\alpha_1 + \mu_H) (\zeta_S + \delta_S + \mu_H) \mathfrak{R}_{HS}} < 0 \quad (3.8)$$

We also observe, from (3.8), that the saturation constant for the cercariae will exert a positive influence in decreasing the weight of schistosomiasis in the populace, regardless of the rates of the additional parameters in the expression on the right flank of (3.8).

$$\frac{\partial \mathfrak{R}_{HS}^2}{\partial L_0} = -\frac{\alpha_1 \beta_J \beta_L \Lambda_H \Lambda_S N_e \phi}{2J_0 L_0 \mu_J \mu_L \mu_s^2 (\alpha_1 + \mu_H)^2 (\zeta_S + \delta_S + \mu_H) \mathfrak{R}_{HS}} < 0 \quad (3.9)$$

We also observe, from (3.9), that the saturation constant for the miracidia will exert a positive influence in decreasing the weight of schistosomiasis in the populace, regardless of the rates of the additional parameters in the expression on the right flank of (3.9). Further analysis of \mathfrak{R}_{HS}^2

yields

$$\lim_{\substack{\zeta_s \rightarrow - \\ N_e \rightarrow 0 \\ \gamma \rightarrow 0}} R_{HS} = 0 \quad (3.10)$$

The limit in (3.10) demonstrates the impact of a schistosomiasis control programme that concentrates on prompt and effective treatment of individuals with active schistosomiasis, reduction of the number of schistosome eggs secreted by infectious humans and reduction of the rate at which eggs secreted by infectious humans successfully become miracidia.

$$\lim_{\substack{\zeta_s \rightarrow - \\ J_0 \rightarrow \infty \\ L_0 \rightarrow -}} R_{HS} = 0 \quad (3.11)$$

The limit in (3.11) demonstrates the impact of a schistosomiasis control programme that concentrates on prompt and effective treatment of individuals with active schistosomiasis and the elimination of both cercariae and miracidia from the aquatic reservoir that hosts them in the environment.

From the analysis of \mathfrak{R}_{HS} as seen in (3.4) - (3.9) and (3.10) - (3.11), respectively, we obtain the following result:

Lemma 3.2. *The effective treatment rate (ζ_s) for the infectious stage of infection of the human sub-population, reduction of both the number of schistosome eggs secreted and the rate at which the secreted eggs successfully become miracidia and the elimination of both cercariae and miracidia from the aquatic reservoir that hosts them in the environment will exert a positive influence in decreasing the schistosomiasis weight in a populace, regardless of the rates of additional parameters in the effective reproduction number.*

Further analysis of the threshold quantity, \mathfrak{R}_{HS} , is carried out by investigating its sensitivity to certain key parameters, namely: the schistosomiasis treatment rate (ζ_s), the cercarial penetration rate (β_J), the number schistosome eggs secreted (N_e), the rate at which the eggs become miracidia (γ) as well as the cercarial production rate (ϕ). Hence, we examine the contour plots (Figures 3 - 6) of \mathfrak{R}_{HS} as functions of ζ_s , β_J , N_e , γ and ϕ . The values of the parameters used for generating the contour plots are obtained from Tables 3 and 4.

Figure 3 suggests that a low rate of cercarial penetration ($\phi = 28\%$) and an average rate at which the schistosome eggs become miracidia ($\gamma = 50\%$) (in the presence of treatment, with $\phi = 500$ and $\gamma = 0.8468$) is needed to annihilate schistosomiasis among the populace. Any regulatory policy dependent on the measures presented in Figure 3 will compel $\mathfrak{R}_{HS} < 1$.

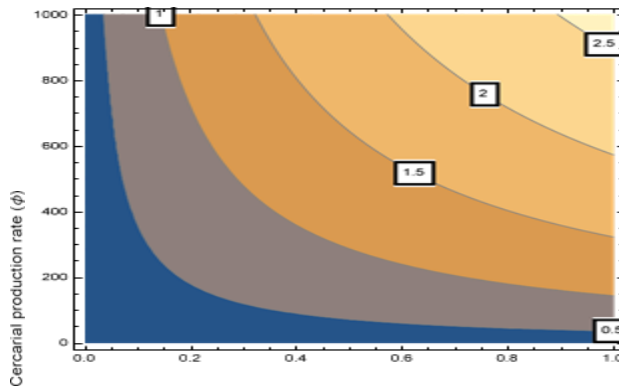


Figure 3: Contour plot consisting of \mathfrak{R}_{HS} dependent on ϕ and γ , when $\phi = 500$ and $\gamma = 0.8468$

Figure 4 shows that an average level of the number of schistosome eggs secreted by humans ($N_e = 40\%$) coupled with an average cercarial production rate ($\phi = 40\%$), in the presence of treatment (with $N_e = 300$ and $\phi = 500$), is required to annihilate schistosomiasis from the populace. Any regulatory policy dependent on the measures presented in Figure 4 will compel $\mathfrak{R}_{HS} < 1$.

Figure 5 suggests that a moderate treatment level of humans with active schistosomiasis ($\zeta_s = 60\%$) coupled with a low schistosomiasis transmission rate ($\beta_I = 1.70$) is needed to annihilate schistosomiasis from the populace. Any regulatory policy dependent on the measures presented in Figure 5 will compel $\mathfrak{R}_{HS} < 1$.

Figure 6 suggests that a high treatment level ($\zeta_s = 60\% - 80\%$) of actively-infected schistosomiasis cases and a low level of cercarial production rate ($\phi = 19\% - 22\%$) are needed to annihilate schistosomiasis from the populace. Any regulatory policy dependent on the measures presented in Figure 6 will compel $\mathfrak{R}_{HS} < 1$.

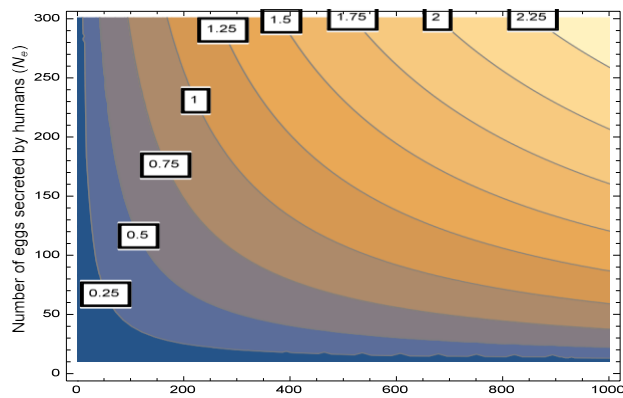


Figure 4: Contour plot consisting of \mathfrak{R}_{HS} dependent on N_e and ϕ

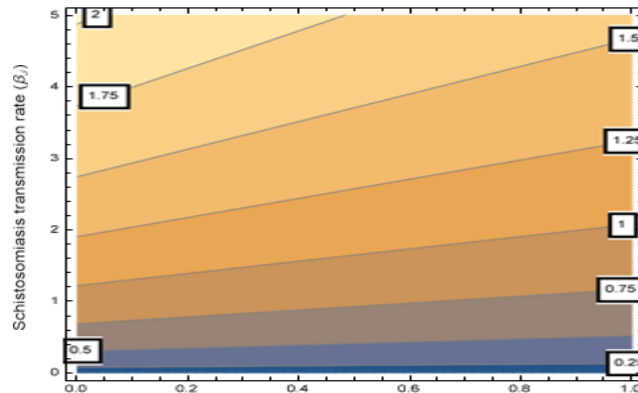


Figure 5: Contour plot of \mathfrak{R}_{HS} dependent on β_I and ζ_s

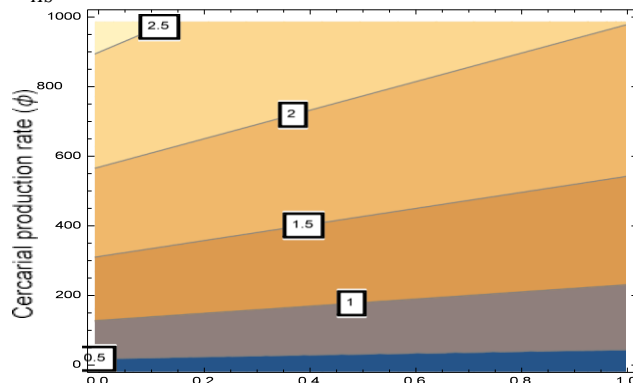


Figure 6: Contour plot of \mathfrak{R}_{HS} , ϕ and ζ_S

4 Uncertainty and Sensitivity Analysis

The model system (2.3) has 57 parameters, and it is expected that uncertainties will occur in estimating parameter rates employed to simulate the model system. To evaluate the extent of these uncertainties and to pin-point those parameters that exert the strongest influence on the population dynamics of tuberculosis-schistosomiasis co-infection, we make use of a technique called *local sensitivity analysis* [19]. Sensitivity analysis decides the influence of model parameters on model conclusions [6, 19]. Local sensitivity investigation demonstrates the impact of a particular parameter while every other parameter is fixed [19]. To achieve this, we compute the sensitivity index, which comprises a partial derivative of the output variable (or function) with respect to the input parameters [6, 9, 19]. Taking the effective reproduction number, \mathfrak{R}_{TS} as the output function and the input parameter to be z_i , the sensitivity index can be calculated as $\partial \mathfrak{R}_{TS} / \partial z_i$ [19]. The normalized sensitivity index $\Omega_{z_i}^{R_{TS}}$, of \mathfrak{R}_{TS} , corresponding to parameter z_i at a fixed rate, z^0 [6,9,19] is

$$\Omega_{z_i}^{R_{TS}} = \frac{\partial \mathfrak{R}_{TS}}{\partial z_i} \times \frac{z_i}{\mathfrak{R}_{TS}} \quad z_i = z^0 \quad (4.1)$$

Using the parameter values in Tables 2 and 3, we proceed to compute the sensitivity indices employing (4.1). We observe that there are twenty-two (22) parameters in the effective reproduction number, $\mathfrak{R}_{TS} = \max\{\mathfrak{R}_{HT}, \mathfrak{R}_{HS}\}$, of the TB-schistosomiasis co-infection system (2.3). We shall investigate the sensitivity of these 22 parameters to \mathfrak{R}_{HT} and \mathfrak{R}_{HS} , respectively.

Table 2: Parameter values (and ranges) of the model (2.3) [1]

Parameters	Values	Sample ranges	References
μ_H	0.02041 year ⁻¹	[0.0143, 0.03]	[38]
Λ_H	3 868 900 year ⁻¹	[3,000,000, 4,000,000]	[12]
β_T	Variable year ⁻¹	[0, 2]	[42]
ξ	0.075 year ⁻¹	[0, 1]	[15]
p	0.1 year ⁻¹	[0, 1]	Assumed
f	0.1 year ⁻¹	[0, 0.005]	[35]
m	0.1 year ⁻¹	[0, 3]	[35]
π_1	0.4 year ⁻¹	[0, 1]	[15]
π_2	0.45 year ⁻¹	[0, 1]	[15]
π_3	0.5 year ⁻¹	[0, 1]	[15]
k_1	0.005 year ⁻¹	[0.005, 0.05]	[5]
k_2	0.005 year ⁻¹	[0.005, 0.05]	[5]
k_3	0.005 year ⁻¹	[0.005, 0.05]	[5]
ζ_T	0.75 year ⁻¹	[0.5, 1]	[27]
ζ_{T1}	0.75 year ⁻¹	[0.5, 1]	[27]
ζ_{T2}	0.75 year ⁻¹	[0.5, 1]	[27]
ζ_{T3}	0.75 year ⁻¹	[0.5, 1]	[27]
ζ_R	0.75 year ⁻¹	[0.5, 1]	[27]
ζ_{R1}	0.75 year ⁻¹	[0.5, 1]	[27]
ζ_S	0.23 year ⁻¹	[0.23, 0.49]	[18]
ζ_{S1}	0.23 year ⁻¹	[0.23, 0.49]	[18]
ζ_{S2}	0.23 year ⁻¹	[0.23, 0.49]	[18]
ζ_{S3}	0.23 year ⁻¹	[0.23, 0.49]	[18]

I.I. Ako - Transactions of NAMP 20, (2024) 45-60

When we consider \mathfrak{R}_{HT} as our output function in (4.1), the two parameters with the highest sensitivity indices were: the rate of TB transmission (β_T) and the rate of TB treatment (ζ_T) (see Table 4 for details). When we consider \mathfrak{R}_{HS} as our output function in (4.1), the thirteen parameters with the highest sensitivity indices were: the snail mortality rate (μ_S), the rate of cercarial infection (β_J), the miracidial infection rate (β_L), the human recruitment rate (Λ_H), the snail recruitment rate (Λ_S), the number of eggs secreted by humans with active schistosomiasis (N_e), the rate at which secreted eggs successfully become miracidia (γ), the rate of cercarial production (ϕ), the saturation constant for cercariae (J_0), the saturation constant for the miracidia (L_0), the natural death rate of humans (μ_H), the cercarial death rate (μ_J), and the miracidial death rate (μ_L) (see Table 5 for details).

Table 3: Parameter values (and ranges) of the model system (2.3) [1] (cont'd)

Parameters	Values	Sample ranges	References
δ_T	0.1 year ⁻¹	[0, 0.5]	[4]
δ_R	0.1 year ⁻¹	[0, 0.5]	[4]
δ_S	1.4 year ⁻¹	[0.365, 2.19]	[23]
α_1	6.5 year ⁻¹	[0, 10]	[23]
α_2	6.5 year ⁻¹	[0, 10]	[23]
α_3	6.5 year ⁻¹	[0, 10]	[23]
ψ	0.85 year ⁻¹	[0.05, 0.85]	Assumed
σ	0.5 year ⁻¹	[0, 1]	Assumed
χ_1	0.65 year ⁻¹	[0, 1]	Assumed
χ_2	0.85 year ⁻¹	[0, 1]	Assumed
η_1	2.0 year ⁻¹	[0, 3]	Assumed
η_2	4.0 year ⁻¹	[0, 5]	Assumed
Θ_{RT}	0.5 year ⁻¹	[0, 1]	Assumed
Θ_{RS1}	1.5 year ⁻¹	[0, 3]	Assumed
Θ_{RS2}	1.5 year ⁻¹	[0, 3]	Assumed
Π_1	1.8 year ⁻¹	[0, 3]	Assumed
Π_2	2.0 year ⁻¹	[0, 3]	Assumed
ν_1	0.001 year ⁻¹	[0, 1]	Assumed
ν_2	0.002 year ⁻¹	[0, 1]	Assumed
ν_3	0.003 year ⁻¹	[0, 1]	Assumed
μ_S	0.5 year ⁻¹	[0, 1]	[18]
Λ_S	73,000 year ⁻¹	[73,000, 109,500]	[10]
ε	182.5 year ⁻¹	[0, 182.5]	[10]
β_L	1.475 year ⁻¹	[0, 2]	Assumed
L_0	10 ⁸ year ⁻¹	[9×10 ⁷ , 1×10 ⁸]	[10]
N_e	300 year ⁻¹	[0, 800]	[10]
γ	0.8468 year ⁻¹	[0, 1]	[10]
μ_L	328.5 year ⁻¹	[100, 400]	[10]
β_J	4.19 year ⁻¹	[0, 5]	Assumed
J_0	9×10 ⁷ year ⁻¹	[8×10 ⁷ , 9×10 ⁷]	[10]
μ_J	3.0 year ⁻¹	[0, 3]	[10]
τ_1	0.1 year ⁻¹	[0, 1]	Assumed
τ_2	0.2 year ⁻¹	[0, 1]	Assumed

ϕ	500 year ⁻¹	[0, 1,000]	[10]
--------	------------------------	------------	------

Table 4: Sensitivity indices for the parameters of the model (2.3) using the effective reproductive number (\mathcal{R}_{HT}) as response function.

Parameters	\mathcal{R}_{HT}
β_T	+1.0000
κ_1	+0.2507
p	+0.0392
μ_H	-0.2741
ζ_T	-0.8617
δ_T	-0.1149

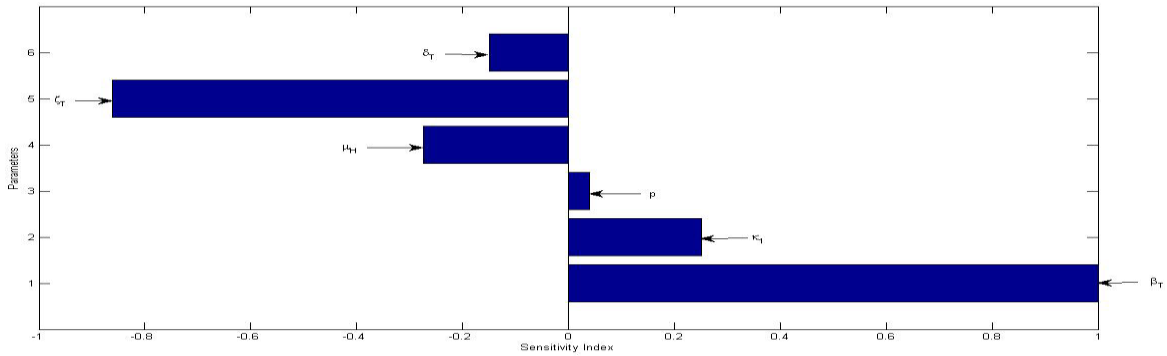


Figure 7: Local sensitivity analysis of \mathcal{R}_{HT}

Table 5: Sensitivity indices for the parameters of the model (2.3) using the effective reproductive number (\mathcal{R}_{HS}) as response function.

Parameters	\mathcal{R}_{HS}	Parameters	\mathcal{R}_{HS}
α_1	+0.0016	J_0	-0.5000
β_J	+0.5000	L_0	-0.5000
β_L	+0.5000	μ_H	-0.5000
Λ_H	+0.5000	μ_J	-0.5000
Λ_S	+0.5000	μ_L	-0.5000
N_e	+0.5000	μ_S	-1.0000
γ	+0.5000	ζ_S	-0.0697
ϕ	+0.5000	δ_S	-0.4241

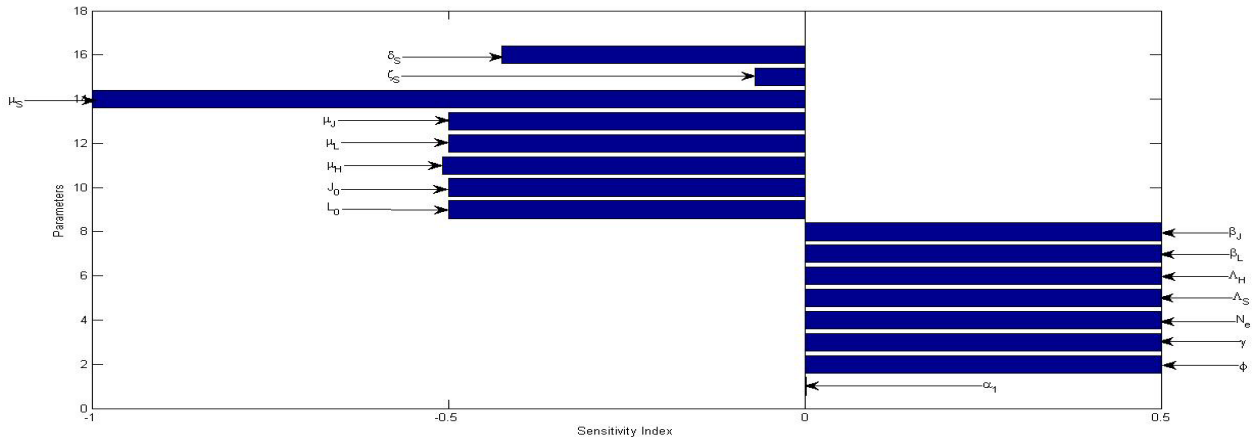


Figure 8: Local sensitivity analysis of \mathcal{R}_{HS}

Conclusion

The analyses of the threshold quantity, \mathfrak{R}_{TS} , was carried out by investigating the sensitivity of its components, \mathfrak{R}_{HT} and \mathfrak{R}_{HS} , respectively to certain key parameters, namely: the treatment rate (ζ_T), the transmission rate (β_T), endogenous reactivation rate (κ_1) as well as the fraction or proportion of fast progressors to TB (p) for the TB component, and the schistosomiasis treatment rate (ζ_S), the cercarial penetration rate (β_J), the number schistosome eggs secreted (N_e), the rate at which the eggs become miracidia (γ) as well as the cercarial production rate (ϕ) for the schistosomiasis component. When we considered \mathfrak{R}_{HT} as our output function in (4.1), the two parameters with the highest sensitivity indices were: the rate of TB transmission (β_T) and the rate of TB treatment (ζ_T). When we chose \mathfrak{R}_{HS} as our output function in (4.1), thirteen parameters with the highest sensitivity indices were: the snail mortality rate (μ_S), the rate of cercarial infection (β_J), the miracidial infection rate (β_L), the human recruitment rate (Λ_H), the snail recruitment rate (Λ_S), the number of eggs secreted by humans with active schistosomiasis (N_e), the rate at which secreted eggs successfully become miracidia (γ), the rate of cercarial production (ϕ), the saturation constant for cercariae (J_0), the saturation constant for the miracidia (L_0), the natural death rate of humans (μ_H), the cercarial death rate (μ_J), and the miracidial death rate (μ_L). With the prior knowledge that it is schistosomiasis infection that drives TB transmission dynamics, and not vice-versa, in a population where they co-infect and co-exist, it is pertinent of all relevant stakeholders in affected areas to pay close and serious attention to all the parameters that drive the perpetuation of both maladies in that population, especially those responsible for the continuance of schistosomiasis in order to eliminate both diseases in the presence of treatment for active TB.

References

- [1] Ako, I.I. and Olowu, O.O. (2024), Causes of Backward Bifurcation in a Tuberculosis-Schistosomiasis Co-infection Dynamics. *Earthline Journal of Mathematical Sciences* 14, Number 4:655–695.
- [2] Athithan, S. and Ghosh, M. (2013). Mathematical modelling of TB with the effects of case detection and treatment, *Int. J. Dynam. Control* 1:223-230, DOI 10.1007/s40435-013-0020-2
- [3] Barbour, A.D. (1982). Schistosomiasis. In: R.M. Anderson (Ed.), *Population Dynamics of Infectious Diseases*, Chapman and Hall, London, pp. 180-208.
- [4] Bhunu, C. P., Garira, W. and Magombedze, G. (2009). Mathematical analysis of a two strain HIV/AIDS model with antiretroviral treatment, *Acta Biotheoretica*, vol. 57, no. 3, pp. 361–381.
- [5] Blower, S. M. McLean, A. R., Porco, T. C., Small, P. M., Hopwell, P. C., Sanchez, M. A. and Moss, A.
- [6] Cariboni, J., Gatelli, D., Liska, R. and Saltelli, A. (2007). The role of sensitivity analysis in ecological modelling, *Ecological modelling* 203 (1-2) 167.
- [7] Castillo-Chavez, C. and Song, B. (2004). Dynamical Models of Tuberculosis and their Applications, *Mathematical Biosciences and Engineering*, Volume 1, Number 2, pp. 361-404.
- [8] Chen Z., Zou L., Shen D., Zhang W. and Ruan S. (2010). Mathematical modelling and control of schistosomiasis in Hubei Province, China, *Acta Tropica* 115, 119-125.

I.I. Ako - Transactions of NAMP 20, (2024) 45-60

- [9] Chitnis, N., Hyman, J.M. and Cushing, J.M. (2008). Determining Important Parameters in the Spread of Malaria Through the Sensitivity Analysis of a Mathematical Model, *Bulletin of Mathematical Biology* 70 (5).
- [10]Chiyaka, E. and Garira, W. (2009). Mathematical analysis of the transmission dynamics of schistosomiasis in the human-snail hosts. *J Biol Syst*; 17:397–423.
- [11]Cohen, J.E. (1977). Mathematical models of Schistosomiasis, *Ann. Rev. Eco. Syst.*, 8, pp. 209–233.
- [12]Countrymeters (2017). Nigeria Population. <https://countrymeters.info/en/Nigeria> (accessed on July 19, 2018).
- [13]Diaby, M., A. and Iggidr, A. (2016). A mathematical analysis of a model with mating structure. *Proceedings of CARI*, 246, pp.402 - 411.
- [14]Diaby, M., A., Iggidr, A., Sy, M., and Sene, A. (2014). Global analysis of a schistosomiasis infection model with biological control. *Applied Mathematics and Computation*, 246, pp.731 - 742.
- [15]Feng, Z., Castillo-Chavez, C. and Capurro, A. F. (2000). A Model for Tuberculosis with Exogenous Reinfection, *Theoretical Population Biology* 57, 235–247
- [16]Feng, Z., Curtis, J. and Minchella, D. J. (2001). The influence of drug treatment on the maintenance of Schistosome genetic diversity. *J. Math. Bio.* 43, 52-68
- [17]Feng, Z., Li, C.-C. and Milner, F. A. (2002). Schistosomiasis models with density dependence and age of infection in snail dynamics. *Math. Biosci* 177-178, 271–286.
- [18]Feng, Z., Eppert, A., Milner, F. A. and Minchella, D. J. (2004). Estimation of Parameters Governing the Transmission Dynamics of Schistosomes. *Applied Mathematics Letters* 17, 1105-1112
- [19]Lutambi, A. M., Penny, M. A., Smith, T. and Chitnis, N. (2013). Mathematical modelling of mosquito dispersal in a heterogeneous environment, *Mathematical Biosciences* 241, 198–216.
- [20]Macdonald, G. (1965). The Dynamics of Helminth Infections with Special Reference to Schistosomes. *Transaction of the Royal Society of Tropical Medicine and Hygiene*. Vol. 59, No. 5, 489-506.
- [21]Milner, F. A. and Zhao, R. (2008). A Deterministic Model of Schistosomiasis with Spatial Structure. *Mathematical Biosciences and Engineering* Vol. 5, No. 3, pp. 505–522, <http://www.mbejournal.org/>
- [22]Mushayabasa, S. and Bhunu, C. P. (2011), Modelling Schistosomiasis and HIV/AIDS Dynamics, *Computational and Mathematical Methods in Medicine*, Vol. 2011, Article ID 846174, doi:10.1155/2011/846174.
- [23]Ngarakana-Gwasira, E. T., Bhunu, C. P., Masocha, M. and Mashonjowa, E. (2016). Transmission dynamics of schistosomiasis in Zimbabwe: A mathematical and GIS Approach, *Commun Nonlinear Sci Numer Simulat* 35, 137-147.

I.I. Ako - Transactions of NAMP 20, (2024) 45-60

- [24] Okosun K. O. and Smith, R. (2017). Optimal Control Analysis of Malaria-Scistosomiasis Co-infection Dynamics, *Math. Bio. & Eng.*, Vol. 14, No.2, pp. 377–405. doi:10.3934/mbe.2017024
- [25] Okuonghae, D. (2013). A mathematical model of tuberculosis transmission with heterogeneity in disease susceptibility and progression under a treatment regime for infectious cases. *Applied Mathematical Modelling* 37, 6786–6808
- [26] Okuonghae, D. (2014), Lyapunov functions and global properties of some tuberculosis models, *J. Appl. Math. Comput.*, DOI 10.1007/s12190-014-0811-4.
- [27] Okuonghae, D. and Aihie, V. (2008). Case detection and direct observation therapy strategy (DOTS) in Nigeria: Its effect on TB dynamics, *Journal of Biological Systems* 16(1):1-31.
- [28] Okuonghae, D. and Aihie, V. U. (2010). Optimal Control Measures for Tuberculosis Mathematical Models Including Immigration and Isolation Of Infective. *Journal of Biological Systems*, 18 (01), 17-54. doi:10.1142/s0218339010003160
- [29] Okuonghae, D. and Ikhimwin, B. O. (2016). Dynamics of a Mathematical Model for Tuberculosis with Variability in Susceptibility and Disease Progressions Due to Difference in Awareness Level. *Front. Microbiol.* 6:1530. doi: 10.3389/fmicb.2015.01530
- [30] Okuonghae, D. and Korobeinikov, A. (2007). Dynamics of Tuberculosis: The effect of Direct Observation Therapy Strategy (DOTS) in Nigeria. *Mathematical Modelling of Natural Phenomena* Vol.2 No.1: Epidemiology pp. 101-113
- [31] Okuonghae, D. and Omosigho, S.E. (2011). Analysis of a mathematical model for tuberculosis: What could be done to increase case detection, *Journal of Theoretical Biology* 269:31–45.
- [32] Olowu, O. and Ako, I. (2023). Computational Investigation of the Impact of Availability and Efficacy of Control on the Transmission Dynamics Schistosomiasis, *International Journal of Mathematical Trends and Technology* Vol. 69 No. 8:1–9.
- [33] Olowu, O., Ako, I. I. and Akhaze, R. I. (2021). Theoretical Study of a Two Patch Metapopulation Schistosomiasis Model, *Transactions of the Nigerian Association Mathematical Physics* Vol. 14 (January - March, 2021 Issue):53–68.
- [34] Olowu, O., Ako, I. I. and Akhaze, R. I. (2021). On the Analysis of a Two Patch Schistosomiasis Model, *Transactions of the Nigerian Association Mathematical Physics* Vol. 14 (January - March, 2021 Issue):69–78.
- [35] Porco, T.C. and Blower, S.M. (1998). Quantifying the intrinsic transmission dynamics of tuberculosis,
- [36] Qi, L. and Cui, J. (2013). A Schistosomiasis Model with Mating Structure, *Abstract and Applied Analysis*, Vol. 2013, Article ID 741386, 9 pages, <http://dx.doi.org/10.1155/2013/41386>
- [37] Qi, L., Xue, M., Cui, J., Wang, Q. and Wang, T. (2018). Schistosomiasis Model and its Control in Anhui Province. *Bulletin of Mathematical Biology* Volume 2014, 80: 2435–2451, <http://doi.org/10.1007/s11538-018-0474-7>

I.I. Ako - Transactions of NAMP 20, (2024) 45-60

- [38]UNAIDS-WHO (2004). *Epidemiological fact sheet*. <http://www.unaids.org>.
- [39]United Nations (2016). Sustainable Development Goals ([https:// sustainable development.un.org/topics/ sustainable development goals](https://sustainabledevelopment.un.org/topics/sustainable-development-goals), accessed 27 July, 2016).
- [40]van den Driessche, P. and Watmough, J. (2002). Reproduction numbers and sub-threshold endemic equilibria for compartmental models of disease transmission, *Mathematical Biosciences* 180: 29–48.
- [41]Waalder, H., Geser, A. and Andersen, S. (1962). The use of mathematical models in the study of the epidemiology of tuberculosis. *Am. J. Public Health Nations Health*. 52(6). pp. 1002–1013.
- [42]World Health Organization (WHO) (2016). Global tuberculosis report 2016. *World Health Organization Press; Geneva, Switzerland*.
- [43]World Health Organization (WHO) (2023). Global Tuberculosis Report 2023. *World Health Organization Press; Geneva, Switzerland*.
- [44]World Health Organization (WHO) (2023). Schistosomiasis Factsheet 2023. *World Health Organization Press; Geneva, Switzerland*.
- [45]Woolhouse, M.E.J. (1991). On the application of mathematical models of schistosome transmission dynamics I: natural transmission, *Acta Trop.*, 49 241.
- [46]Zhao, R. and Milner, F. A. (2008). A mathematical model of *Schistosoma mansoni* in *Biomphalaria glabrata* with control strategies, *Bulletin of Mathematical Biology*, vol. 70, no. 7, pp. 1886–1905.